

Azacalix[3]arene–Carbazole Conjugated Polymer Network Ultrathin Films for Specific Cation Sensing

Chatthai Kaewtong,^{†,‡} Guoqian Jiang,[†] Yushin Park,[†] Tim Fulghum,[†] Akira Baba,[†] Buncha Pulpoka,^{*,‡} and Rigoberto Advincula^{*,†}

Department of Chemistry and Department of Chemical Engineering, University of Houston, 136 Fleming Building, Houston, Texas 77204-5003, and Department of Chemistry, Faculty of Science, Chulalongkorn University, Bangkok 10330, Thailand

Received January 28, 2008. Revised Manuscript Received May 8, 2008

Developing highly selective and sensitive chemical sensors is a challenge with respect to new materials for chemical recognition. In this study, a new conjugated polymer network precursor, hexahomotriazacalix[3]arene–carbazole has been synthesized and electrochemically cross-linked to form ultrathin films using cyclic voltammetry. The incorporation of hexahomotriazacalix[3]arene moiety as a neutral cation-binding receptor into a conjugated polycarbazole network facilitates high selectivity and sensitivity for Zn^{2+} . The ultrathin films were characterized spectroscopically using UV–vis absorption and fluorescence spectroscopy. Surface morphology properties were examined by atomic force microscopy. Electrochemical deposition parameters and sensor transduction was studied by an electrochemical quartz crystal microbalance, surface plasmon resonance spectroscopy, and open-circuit potentiometry techniques. The results indicate that the high selectivity and sensitivity for Zn^{2+} compared to those of other cations is due to the combined size and dipole specificity of the azacalixarene unit and nonspecific ionic interaction with the redox couple of the conjugated polycarbazole units.

Introduction

The basic recognition element of a chemical sensor is essentially a molecular or macromolecular structure designed to recognize a specific analyte. The binding or complexation constant, K_{asso} , of the analyte is dependent on the strength of noncovalent interaction and accessibility to this structure. A high surface area is also a factor as it affects the diffusion kinetics of the analyte to the binding site. In the presence of a conducting (π -conjugated) polymer, a polymeric chemosensor system can be made electrochemically active, electrically conducting, and fluorescent, depending on the structure of the polymer, mode of electric field application, and wavelength excitation. Thus, it is not necessary for the receptor-analyte unit of the polymeric chemosensor to have an inherently high K_{asso} . Only partial occupancy of the recognition site may be required for signal transduction since the conjugated polymer also contributes to signal amplification and improved sensitivity.¹

A number of well-investigated π -conjugated polymers such as polythiophenes, polypyroles, polyanilines, etc. have been used successfully for sensor and device applications.² As a class of semiconducting polymers, polycarbazoles possess good electroactivity and useful thermal, electrical, and photophysical properties which have led to their use in

redox catalysis, electrochromic displays, electroluminescent devices, and sensors.³ For example, polycarbazole has been used to develop copper(II) ion-selective microelectrochemical transistors^{4a} and L-dopa-selective sensors^{4b} due to its negligible sensor response hysteresis and greater chemical and thermal stability compared to other conducting polymers.⁴

Calixarenes have received significant attention for the construction of molecular receptors due to their unique molecular recognition properties and ease of functionalization.⁵ The size of the macrocyclic cavity and the presence of ion–dipole interactions with the heteroatoms can be made specific for a particular ion. Substituents to the calixarene can further control the size and specificity of the cavity through conformational change (torsional) and electronic effects. In recent years, oxacalixarenes and azacalixarenes have been developed as part of a class of compounds called expanded calixarenes.⁶ The azacalixarenes, which have nitrogen atoms in the macrocyclic ring, could provide additional binding sites for many types of cations. Specifically, the azacalix[3]arenes have been shown to serve as

- (2) (a) Richard, D. M. *Adv. Mater.* **1998**, *10*, 93. (b) Roncali, J. *J. Mater. Chem.* **1999**, *9*, 1875. (c) Janata, J.; Mira, J. *Nat. Mater.* **2003**, *2*, 19. (d) Bobacka, J.; Ivaska, A.; Lewenstam, A. *Electroanalysis* **2003**, *15*, 366.
- (3) (a) Mallouk, T. E.; Gavin, J. A. *Acc. Chem. Res.* **1998**, *31*, 209. (b) Crooks, R. M.; Ricco, A. J. *Acc. Chem. Res.* **1998**, *31*, 219.
- (4) (a) Rani, V.; Santhanam, K. S. V. *J. Solid State Electrochem.* **1998**, *2*, 99. (b) Kawde, R. B.; Laxmeshwar, N. B.; Santhanam, K. S. V. *Sens. Actuators B* **1995**, *23*, 35. (c) Choudhury, S.; Saxena, V.; Gupta, S. K.; Yakhmi, J. V. *Thin Solid Films* **2005**, *493*, 267.
- (5) (a) *Calixarenes in Action*; Mandolini, L., Ungaro, R., Eds.; Imperial College Press: London, U. K., 2000. (b) Ikeda, A.; Shinkai, S. *Chem. Rev.* **1997**, *97*, 1713. (c) Vigalok, A.; Zhu, Z.; Swager, T. M. *J. Am. Chem. Soc.* **2001**, *123*, 7917. (d) Vigalok, A.; Swager, T. M. *Adv. Mater.* **2002**, *14*, 368.

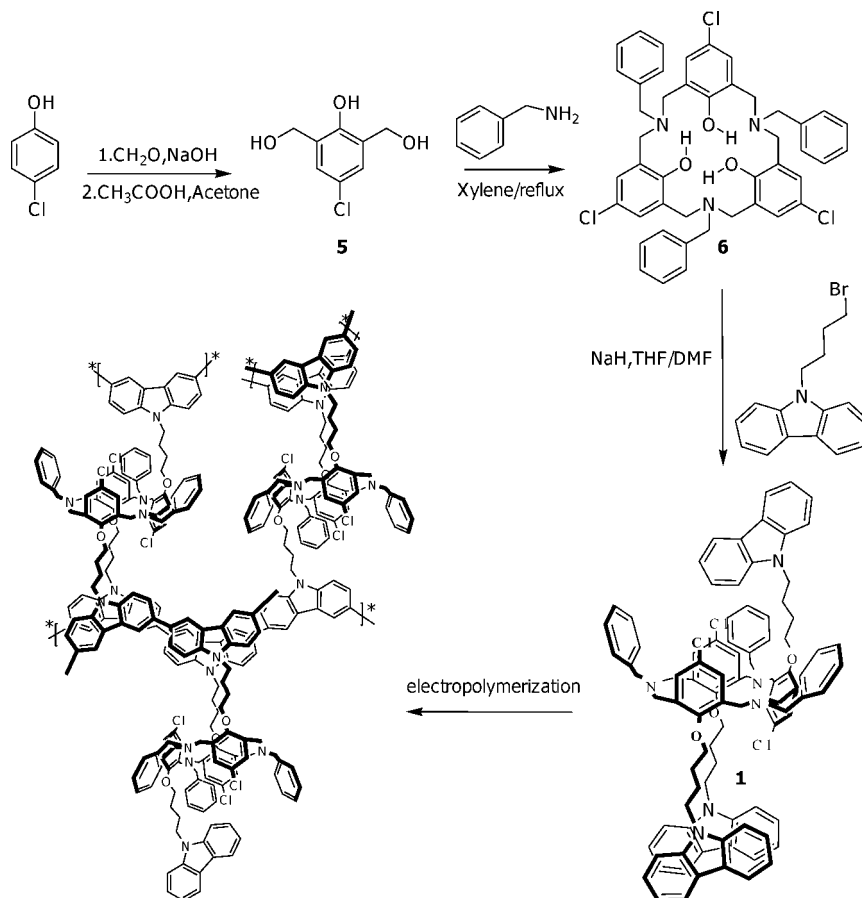
* Authors to whom correspondence should be addressed. E-mail: radvincula@uh.edu (R.A.); buncha.p@chula.ac.th (P.B.).

[†] University of Houston.

[‡] Chulalongkorn University.

(1) (a) Swager, T. M. *Acc. Chem. Res.* **1998**, *31*, 201. (b) Dimitriev, O. P. *Macromolecules* **2004**, *37*, 3388. (c) Ferguson, G.; Gallagher, J. F.; Lough, A. J.; Notti, A.; Pappalardo, S.; Parisi, M. F. *J. Org. Chem.* **1999**, *64*, 5876.

Scheme 1. Synthesis and Electrochemical Polymerization (Cross-linking) of *p*-Chloro-*N*-benzylhexahomotriazacalix[3]-tri(buthyl carbazole) or Monomer



highly selective receptors for both cations^{6d,e} and anions.⁷ Halide anion selectivity can be tuned by first complexing a cation with bridged nitrogen atoms inside the macrocycle.⁷

With the aim of preparing a new class of chemical recognition elements for sensors, we have synthesized hexahomotriazacalix[3]arene-carbazole as a precursor for the formation of conjugated polymer networks (CPN). To the best of our knowledge, there has been no report on the use of azacalix[3]arene in partial-cone conformation combined with polycarbazoles in a chemical sensor material system. By electropolymerization, these precursors can be deposited as ultrathin films on Au and indium tin oxide (ITO) electrode substrates. This electrochemical process results in the formation of a CPN due to the inherent intermolecular and intramolecular reactivity of pendant carbazole units.⁸ The films were characterized by UV-vis spectroscopy, fluorescence spectroscopy, and atomic force microscopy (AFM).

The electrochemical and sensing properties were investigated in conjunction with various electrochemically hyphenated optical and acoustic techniques, e.g., electrochemical quartz crystal microbalance (EC-QCM), electrochemical surface plasmon spectroscopy (EC-SPR), and open-circuit potentiometry. It is believed that the partial-cone conformation of azacalix[3]arene allows a gain in the kinetic binding property, with its selectivity remaining intact with electropolymerization, leading to a high specificity for Zn^{2+} .

Results and Discussion

Synthesis. The synthesis of monomer **1** Scheme 1 was completed by reacting *N*-benzylhexahomotriaza-*p*-chlorocalix[3]arene^{6e} with 3.5 equiv of 9-(4-bromobutyl)-9*H*-carbazole and 3.5 equiv of NaH as base in THF/DMF solution for 2 days. Column chromatography (silica gel, 90/10 hexane/ethyl acetate) was used to afford monomer **1** in 10% yield. The carbazole-functionalized hexahomotriazacalix[3]arene monomer was then characterized by FT-IR, ¹H NMR, ¹³C NMR, and MALDI-TOF MS as summarized in the Experimental Section.

It was found that hexahomotriazacalix[3]-tricarbazole **1** was fixed as a partial-cone conformation as evidenced by the presence of two triplet $-CH-$ azacalix aromatic peaks at 7.04 ppm ($J = 7.2$ Hz) and 7.01 ppm ($J = 7.2$ Hz) and multiplet peaks of $-NCH_2Ar-$ at 3.78–3.00 ppm in the ¹H NMR spectrum. The ¹³C NMR spectrum also gave evidence of the changes,

(6) (a) *Calixarenes 2001*; Asfari, Z.; Bhmer, V.; Harrowfield, J.; Vicens, J., Eds.; Kluwer Academic Publishers: Dordrecht, 2001. (b) Takemura, H. *J. Inclusion Phenom. Macro.* **2002**, *42*, 1698. (c) Takemura, H.; Shimmyozu, T.; Inazh, T. *Coord. Chem. Rev.* **1996**, *156*, 183. (d) Hampton, P. D.; Tong, W.; Wu, S.; Duesler, E. N. *J. Chem. Soc., Perkin Trans. 1996*, *2*, 1127. (e) Thury, P.; Nierlich, M.; Vicens, J.; Takemura, H. *J. Chem. Soc., Dalton Trans.* **2000**, 279.

(7) Kaewtong, C.; Fuangswasdi, S.; Muangsri, N.; Chaichit, N.; Vicens, J.; Pulpoka, B. *Org. Lett.* **2006**, *8*, 1561.

(8) (a) Taranekar, P.; Baba, A.; Fulghum, T. M.; Advincula, R. *Macromolecules* **2005**, *38*, 3679. (b) Baba, A.; Onishi, K.; Knoll, W.; Advincula, R. *J. Phys. Chem. B* **2004**, *108*, 18949. (c) Taranekar, P.; Fulghum, T. M.; Baba, A.; Patton, D.; Advincula, R. *Langmuir* **2007**, *23*, 908.

consistent with the previous study from a cone conformation spectrum,⁷ i.e., $-\text{OCH}_2\text{CH}_2-$ showed two peaks (75.0, 74.7 ppm) and the $-\text{C}-$ of the aromatic azacalix split into three peaks (135.0, 134.0, and 133.5 ppm).

Electropolymerization of *p*-Chloro-*N*-benzylhexahomotriazacalix[3]-tri(butyl carbazole). Electropolymerization by cyclic voltammetry (CV) is a widely used method for preparing polycarbazole (PCBz) films.^{9,10} To test the ability to form network ultrathin films, monomer **1** was electropolymerized and deposited on three working electrodes: plain gold-coated glass substrate, CBzC11SH (thiol-undec-9H-carbazole) (**4**) self-assembled monolayer (SAM) coated gold substrate, and ITO substrate. All the CV trace diagrams of monomer **1** deposited onto the different substrates are also shown in Figure S3 (Supporting Information). Deposition on a bare gold-coated slide was first attempted. The current increase was low and the CV was not well-behaved. When the **4** SAMs coated gold substrate was used (Figure 1a), the monomer was shown to be electropolymerized anodically at 1.0 V. After several cycles, the oxidation and reduction peaks were observed at 0.85 and 0.77 V, respectively. The current was low on the first cycle but increased in the second and slightly changed with further cycles. Thus, compared to the bare-Au electrode, more material was deposited on this **4** coated gold substrate based on a higher current increase at 0.85 V. On the other hand, the best films were obtained when ITO was used as the electrode-substrate with an applied potential window from 0 to 1.3 V (Figure 1b) (electropolymerization was initially attempted with applied potential up to 1.5 V, Figure S3). The linear increase in the oxidation current and high cyclic reversibility is indicative of uniform film growth. The anodic current trace splits into two peaks with further cycles. At the first cycle, the broad anodic peak is centered at 0.90 V and the reduction peak is at 0.75 V. When the eighth cycle was reached, two consecutive anodic peaks centered at 0.85 and 0.96 V became more pronounced. The two anodic current peaks can be assigned to the doping with anions into the polymerized carbazole from the electrolyte solution and oxidation of the remaining carbazole monomer, leading to radical cation species.⁸ This is reasonable because only one reduction peak is observed, which decreases from 0.75 to 0.71 V. Thus, the reduction from the previously oxidized but un-cross-linked species may be the source of this peak. Dedoping may also be involved in this reduction process but is not favored considering polycarbazole is a p-type semiconductor polymer.

Morphology Studies. The morphology before and after electropolymerization on the ITO, gold-coated slides and **4** SAM coated gold substrates were characterized by AFM

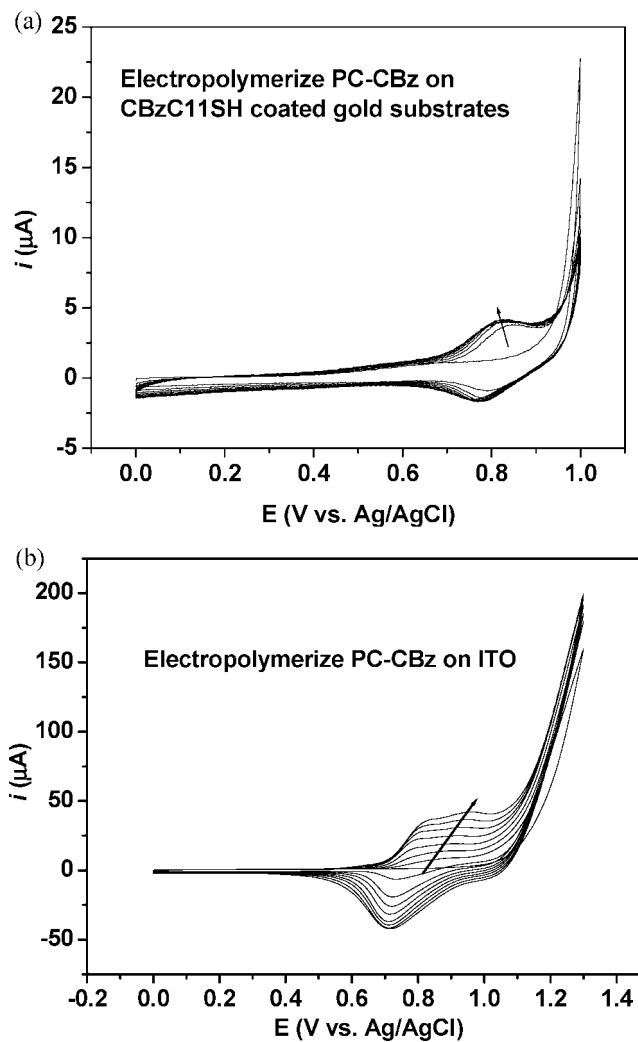


Figure 1. Cyclic voltammograms of the electrochemical cross-linking/deposition of PC-CBz at a scan rate of 50 mV/s, 8 cycles: (a) deposited material on **4** coated gold substrates and (b) deposited material on ITO substrates.

(Figure 2). All the other AFM images are shown in Figures S4 and S5 (Supporting Information). PC-CBz was electropolymerized for 8 cycles at a range of 0–1.0 V with a scan rate of 50 mV/s in 0.1 M TBAPF₆/anhydrous CH₂Cl₂ as electrolyte (WE, gold-coated slide; CE, Pt wire; RE, Ag/AgCl wire). In the case of direct deposition on unfunctionalized gold substrate, the morphology was found to be more similar to that of bare gold, indicating a very small quantity was deposited. When **4** SAM coated gold was used, the morphologies are relatively rough (rms roughness = 15 nm) (Figure 2a, b). It implied that the deposition of the precursor material was achieved better on **4** coated gold substrates but were not as uniform as expected. The nucleation of **4** SAM may play a very important role during the polymerization, as suggested from a previous report on polythiophene electrodeposition.¹¹ For the ITO substrates, a highly uniform morphology (rms roughness = 7 nm) was observed with applied potentials from 0 to 1.3 V (Figure 2c, d). However, in the case of higher applied potential (up to 1.5 V), the polymer films tended to give a rougher and patchy film (but

(9) (a) Kuwabara, Y.; Ogawa, H.; Inada, H.; Nona, N.; Shirota, Y. *Adv. Mater.* **1994**, *6*, 667. (b) O'Brien, D. F.; Burrows, P. E.; Forrest, S. R.; Koene, B. E.; Loy, D. E.; Thompson, M. E. *Adv. Mater.* **1998**, *10*, 1108. (c) Koene, B. E.; Loy, D. E.; Thompson, M. E. *Chem. Mater.* **1998**, *10*, 2235. (d) Thomas, K. R. J.; Lim, J. T.; Tao, Y. T.; Ko, C. W. *J. Am. Chem. Soc.* **2001**, *123*, 9404. (e) Li, J.; Liu, D.; Li, Y.; Lee, C. S.; Kwong, H. L.; Lee, S. *Chem. Mater.* **2005**, *17*, 1208.

(10) (a) Liu, B.; Yu, W. L.; Lai, Y. H.; Huang, W. *Chem. Mater.* **2001**, *13*, 1984. (b) Xia, C.; Advincula, R. C. *Macromolecules* **2001**, *34*, 5854. (c) Stephen, O.; Vial, J.-C. *Synth. Met.* **1999**, *106*, 115.

(11) Kang, J. F.; Perry, J. D.; Tian, P.; Kilbey, S. M. *Langmuir* **2002**, *18*, 10196.

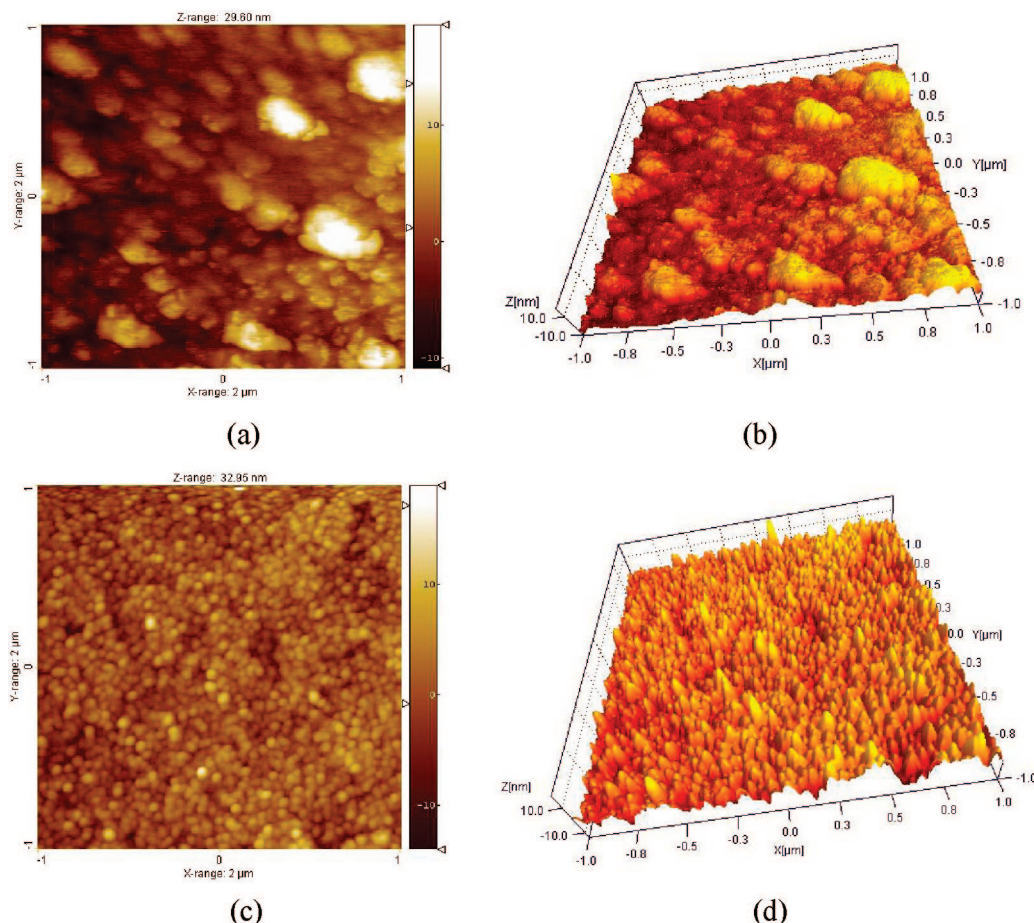


Figure 2. 2D (a, c) and 3D (b, d) AFM images of PPC-CBz electropolymerized at 50 mV/s in $\text{TBAPF}_6/\text{CH}_2\text{Cl}_2$ electrolyte (CE, Pt wire; RE, Ag/AgCl wire): on the **4** coated gold substrate (WE) (rms roughness = 15 nm) (a, b) and on the ITO substrate (WE) (rms roughness = 7 nm) (c, d).

complete coverage) as shown in Figure S5 (Supporting Information).

Spectroelectrochemistry. Spectroelectrochemical measurements were performed using a previously described setup.¹² The spectroelectrochemical measurement of PPC-CBz was performed to investigate the cross-linking polymerization process *in situ* and the presence of polaronic states associated with the formation of a more conjugated polymer. The *in situ* UV-vis absorption spectra of PC-CBz were measured simultaneously with electropolymerization in a 0.1 M $\text{TBAPF}_6/\text{CH}_2\text{Cl}_2$ solution as electrolyte (WE, ITO; CE, Pt wire; RE, Ag/AgCl) at a scan rate of 50 mV/s. Figure 3 shows the extended appearance of the $\pi-\pi^*$ transition peak and a shoulder at 445 nm, which is attributed to polycarbazole.¹³ The broad peak centered at 950 nm can be assigned to the polaronic and bipolaronic bands originating from the formation of the conjugated polycarbazole species and their complexed ion redox couple with hexafluorophosphate ions. From the spectra, the peaks at 445 and 950 nm were tracked and showed a linear increase with increasing CV cycles, indicating an even deposition of the polymer.

In addition to the electronic absorption properties, the fluorescence emission properties of polycarbazole further

confirmed the cross-linking reaction.¹⁴ It was found that the azacalix[3]arene–carbazole precursor shows different fluorescence spectra before and after cross-linking. The fluorescence peak of the carbazole units present on PC-CBz was observed at 370 nm (Figure 3b) (film). After electropolymerization, this peak is quenched in the case of the solid state PPC-CBz film, where a new peak arises at 390 nm attributed to the formation of polycarbazole. This was also observed previously as in the case of CBz functionalized polybenzyl ether dendrimers in solution and solid-state carbazole containing polystyrenic CPN films.¹⁴

Sensing Selectivity and Sensitivity: Potentiometric Measurements. The sensing selectivity and sensitivity studies were first investigated by open-circuit potentiometry (an electrochemical cell potential set at zero current). The changes in potential (ΔE) were recorded simultaneously as a function of time at constant zero-current voltage. The experiment also tracks the redox state of the polymer since it can be influenced by either introducing an electric charge or adding a reagent (analyte) which interferes with the redox equilibrium. The selectivity studies by potentiometry were first performed using the electrochemically cross-linked PPC-CBz film on ITO against 10^{-6} M of the various cations (0.01 M TBACl is present as supporting electrolyte).

(12) Tran-Van, F.; Chevrot, C. *Electrochim. Acta* **2002**, *47*, 2927.

(13) (a) Buttry, D. A. In *Electroanalytical Chemistry*; Bard, A. J., Ed.; Marcel Dekker: New York, 1991; Vol. 17, p 1. (b) Taranekar, P.; Baba, A.; Fulghum, T.; Advincula, R. *Macromolecules* **2005**, *38*, 3679.

(14) Taranekar, P.; Park, J.-Y.; Patton, D.; Fulghum, T.; Ramon, G. J.; Advincula, R. *Adv. Mater.* **2006**, *18*, 2461.

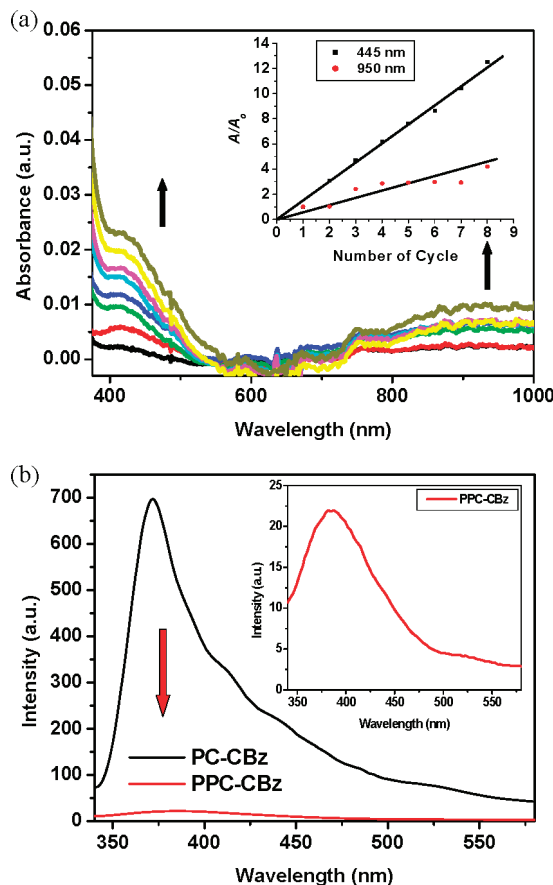


Figure 3. (a) Spectroelectrochemical analysis performed in 0.1 M TBAPF₆/CH₂Cl₂ of PC-CBz, growth of the 445 and 950 nm peaks during electrodeposition of PPC-CBz, spectra taken in situ at 0 V during each CV cycle and (b) fluorescence spectra before and after electropolymerization of PC-CBz which are taken at the excitation wavelength $\lambda = 320$ nm.

As shown in Figure 4a, the highest selectivity (biggest change in ΔE of up to -0.06 V) was observed from Zn²⁺ compared with those of other cations. A priori, this may be due to the exact size and fit of the Zn²⁺ cation on the azacalix[3]arene, steric effect from the polymer backbone and hard–soft acid and base principle (HSAB).⁶ The presence of the nitrogen atoms (soft) in azacalix[3]arenes allows them to bind soft cations (such as transition metals).^{6e,7} However, our previous work⁷ has shown that the azacalix[3]arene template can be made specific for Zn²⁺ ions in organic solution. Thus, by design, the hexahomotriazacalix[3]-tri(butylcarbazole) was made to be specific for the Zn²⁺ cations compared to the other transition metals. In this case, the conductivity of the cross-linked polymer may increase with binding of the Zn²⁺ cations to the azacalix[3]arene pocket. This seemed to be readily achieved at 10^{-6} M where the other cations have little effect on the potential change since they did not have an exact fit on the azacalix[3]arene units and thus showed little deviation from the zero-current potential.

In general for the Zn²⁺ cations, after the lowest concentration (10^{-6} M), the ΔE did not decrease much over time (Figure 4b). For the other concentrations, the potential decreases in the first 100 s, followed by a gradual increase until it reaches a steady state. This is generally observed for all the other cations at higher concentrations (10^{-5} to 10^{-3}

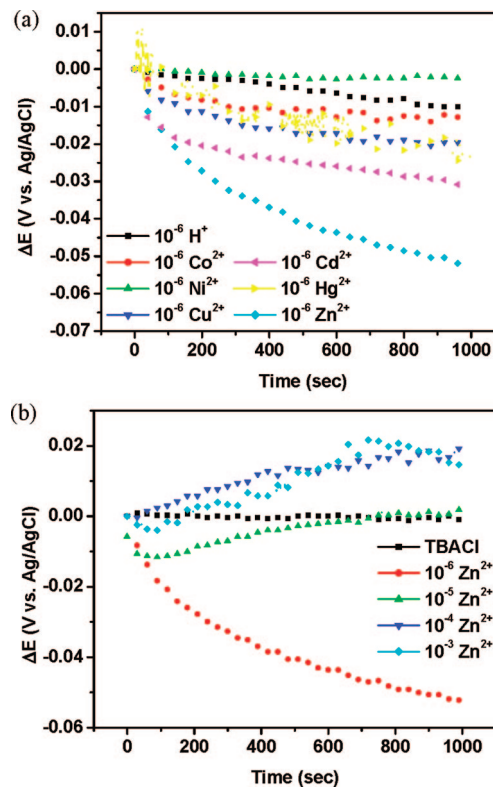
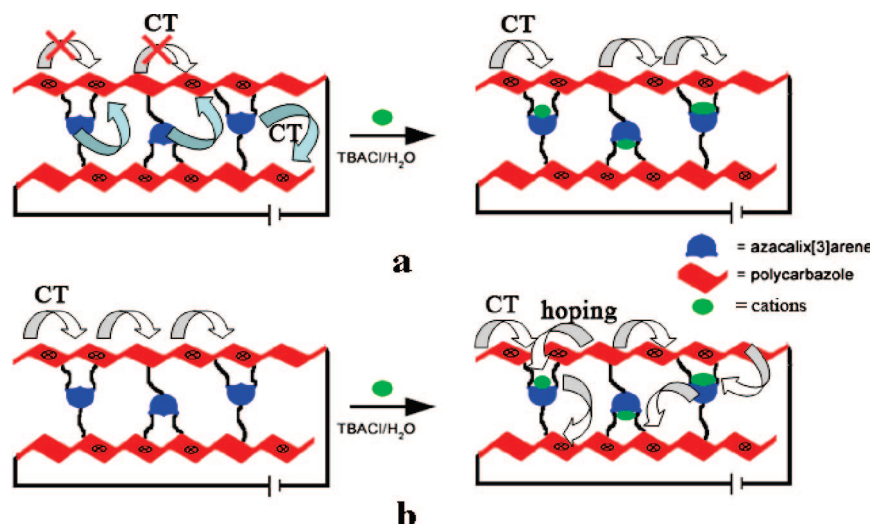


Figure 4. Potentiometric profiles of PPC-CBz on ITO in 0.01 M TBACl aqueous solution: (a) various cation analytes and (b) various concentrations of Zn²⁺. Plotted data are within 5% deviation from several measurements.

M) (see Figure S6, Supporting Information). This indicates that the decrease of potential at 10^{-6} M of the cations over time is primarily due to the first cations being encapsulated in the cavity of azacalix[3]arene through cation–dipole interaction. With increasing concentrations, the limited amount of the cavities does not allow further encapsulation and therefore cations are free to complex with other species in the polymer backbone, i.e., driven by the interaction between the cations with doped anions (Cl[−] and PF₆[−]) along the extended π -conjugated polymer backbone. Thus, the potentiometric changes can be attributed to the increasing interference of the Zn²⁺ on charged species in the polymer such as polarons and bipolarons along with their neutralizing counterions which are independent species.

Clearly, on the basis of the potentiometric measurements in the presence of 10^{-6} M cations, the Zn²⁺ showed the best performance in terms of selectivity and sensitivity compared to the other cations. However, there is a need to further explain this phenomenon of the ΔE change beyond the HSAB principle and the presence of other independent ionic species in the polymer. The basic premise is that the other ions when not bound to the azacalix[3]arene cavity via a cation–dipole interaction are primarily involved with ion pairing on the doped conjugated polymer, i.e., cation– π interaction between cations and π -extended conjugated polymer.

To begin with, the observed behavior can be correlated with the effect of charge-carrier properties on a conjugated polymer, i.e., hole transport and electron transfer properties of the polycarbazole to the cations. There are two explana-

Scheme 2. Two Explanations for the Potential Changes after the Addition of Different Cations^a

^a (a) Cations can be protected from electron transfer to the conjugated polymer backbone and (b) cations complexation can be a hole to improve the hole transport pathways between chains.

tions for the potential changes after the addition of different cations along with different concentrations: (1) One can first consider the contribution of electron transfer from the lone pair of nitrogen on the azacalix[3]arene moiety to the conjugated polymer backbone. This was confirmed by studying the complexation of protons with the azacalix[3]arene (see Figure S6a, Supporting Information). As shown in Scheme 2a, protonation of nitrogen (ammonium formation) induces less efficiency for electron transfer to the polycarbazole. As a consequence, fewer holes can be generated and thus less conductivity enhancement or a smaller potential decrease would be expected, which is indeed the case. (2) The other consideration is based on hole transport throughout the whole polymer network in a three-dimensional manner. Since the Zn^{2+} are complexed in the azacalix[3]arene cavities by ion–dipole interaction as shown in Scheme 2b, the holes not only move along the polymer backbones but also hop through the cations to improve the hole transport pathways between chains.^{15a} The other effect to consider is the competition with the free ions (overall ionic strength) and the ions bound on the doped polymer. With increasing concentration of the cations, the ion–ion and cation– π interactions increases and begin to reside proximal to the polymer backbones, pairing with the anions (Cl^- and PF_6^-) on the doped sequences of the polymer. Thus, they tend to decrease the doping level of the polymer films by removing the anions paired to the polymer backbone and thus the stabilization of π -extended conjugated polymer chains.

Consequently, the net potential shift is attributed to the competition of these two effects. The flux of the cations into the polymer films may proceed in two steps: at first they diffuse into the polymer and selectively bind with the azacalix[3]arene cavities, which enhances the conductivity. If all the cavities have been filled up, the cations would slowly disperse to the sequences occupied by the dopants, which interrupts the polymeric conjugation and decreases the hole mobility.

In principle, the conductivity of conjugated polymers can be fine-tuned by changing charge transport pathways. Previous studies¹⁵ correlated that the three-dimensional connectivity for bipolaron migration was caused by the close contact between planar π -extended polymers which efficiently promote an interstrand charge hopping mechanism and consequently facilitates charge delocalization. On the other hand, the minimization of cross-communication of the conjugated polymer backbones can remarkably change the conductivity profile by reducing the dimensionality of charge-transporting pathways.¹⁶ As a control experiment, 9-(4-(9H-carbazol)-9H-carbazole (**8**) was used. The data showed only a little change in ΔE as shown in Figure S7 (Supporting Information) at -0.004 V compared to -0.06 V in the absence of the azacalix[3]arene units.

Spectroelectrochemical studies were also performed to support the order of cation sensitivity and selectivity. As expected, the addition of 10^{-3} M cations into the cell containing the films resulted in different changes in the absorption spectra. The blue shift (≈ 45 nm) from 455 nm to 405 nm and 950 nm to 910 nm upon the addition of Ni^{2+} , Cu^{2+} , Cd^{2+} , and Hg^{2+} suggests that conjugation of the polycarbazole indeed decreased, consistent with the above discussion in the potentiometric measurements. However, little change in the absorption spectra of **1** was observed upon the addition of Zn^{2+} and Co^{2+} and can be attributed primarily to an allosteric effect. This suggests that the Zn^{2+} and Co^{2+} ions are primarily bound in the cavity of azacalix[3]arene by cation–dipole interaction. This was also confirmed by the addition of protons. As can be seen from Figure 5, there is a slight blue shift with protons primarily bound on the nitrogen of azacalix[3]arene, but the interference is much weaker than the metal ions, maintaining the polymeric

(15) (a) Zhu, S. S.; Swager, T. M. *J. Am. Chem. Soc.* **1997**, *119*, 12568. (b) Lee, D.; Swager, T. M. *J. Am. Chem. Soc.* **2003**, *125*, 6870.

(16) (a) Miller, L. L.; Mann, K. R. *Acc. Chem. Res.* **1996**, *29*, 417. (b) Cornil, J.; Beljonne, D.; Calbert, J.-P.; Brédas, J.-L. *Adv. Mater.* **2001**, *13*, 1053.

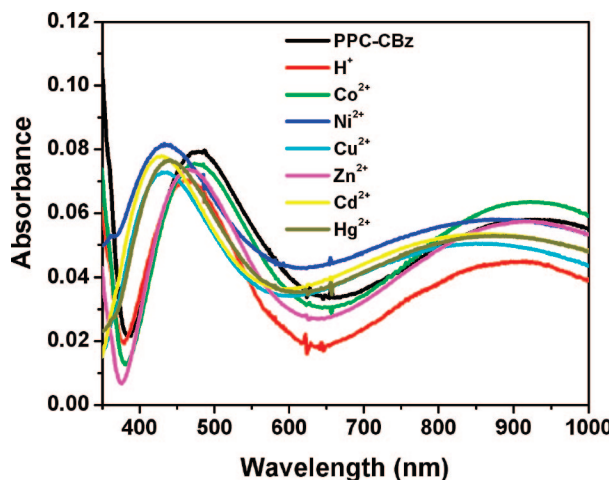


Figure 5. UV-vis absorption spectrum of PPC-CBz films upon the addition of different cations with the concentration 10^{-3} M on ITO substrates.

conjugation to a large extent. From the Co^{2+} spectrum, this may imply that Co^{2+} ion may compete with Zn^{2+} for the azacalix[3]arene specificity. However, the blue shift (~ 10 nm) from 450 to 440 nm occurred upon the addition of Zn^{2+} in the control experiment (Figure S7b). From this data, the blue shift can be explained by cation- π interactions between the cations and the conjugated polymers.

Additionally, we used a combined electrochemistry and quartz crystal microbalance method (EC-QCM) to confirm the sensitivity and selectivity of PPC-CBz. This method is very informative for probing mass-transport processes in thin films.¹² The mass deposition per cycle was measured during electropolymerization and showed a general decrease in frequency with each cycle over time, indicating a continuous deposition on the substrate (Figure 6a). After the deposition of PPC-CBz on the EQCM probe, aqueous solutions of the cations were added. In general, the Butterworth-van Dyke (BD) equation provides a method for relating the electrical properties of the quartz resonator to the mechanical properties of the deposited film.¹⁷ The relationship between ΔR and ΔF under liquid loading was derived from the BD equation.¹⁸ The increase in ΔR is correlated with an increase in the viscoelasticity of the layer adjacent to the crystal surface while a small change in ΔR is indicative of a more rigid adsorbed layer. From Figures 6a and 6b, the resistance increased with each cycle, indicating increasing rigidity (viscoelastic behavior) of the films with more layers deposited. In general, with oxidation and reduction, the change in resistance indicates the transport of the ions in and out of the cross-linked film. After cross-linking, the addition of Zn^{2+} caused a rapid increase of the mass of the deposited polymer (Figure 6c). This was the highest for the Zn^{2+} as compared to the other ions. Analysis of the mass-concentration relationship, according to the Langmuir equation ($1/\Gamma = 1 + 1/KC_M$, where $\Gamma = \Delta m/\Delta m_{\text{max}}$, C_M is the metal ion concentration and K the complexation constant) was made.¹⁹ The binding ability of PPC-CBz toward cations thus varies

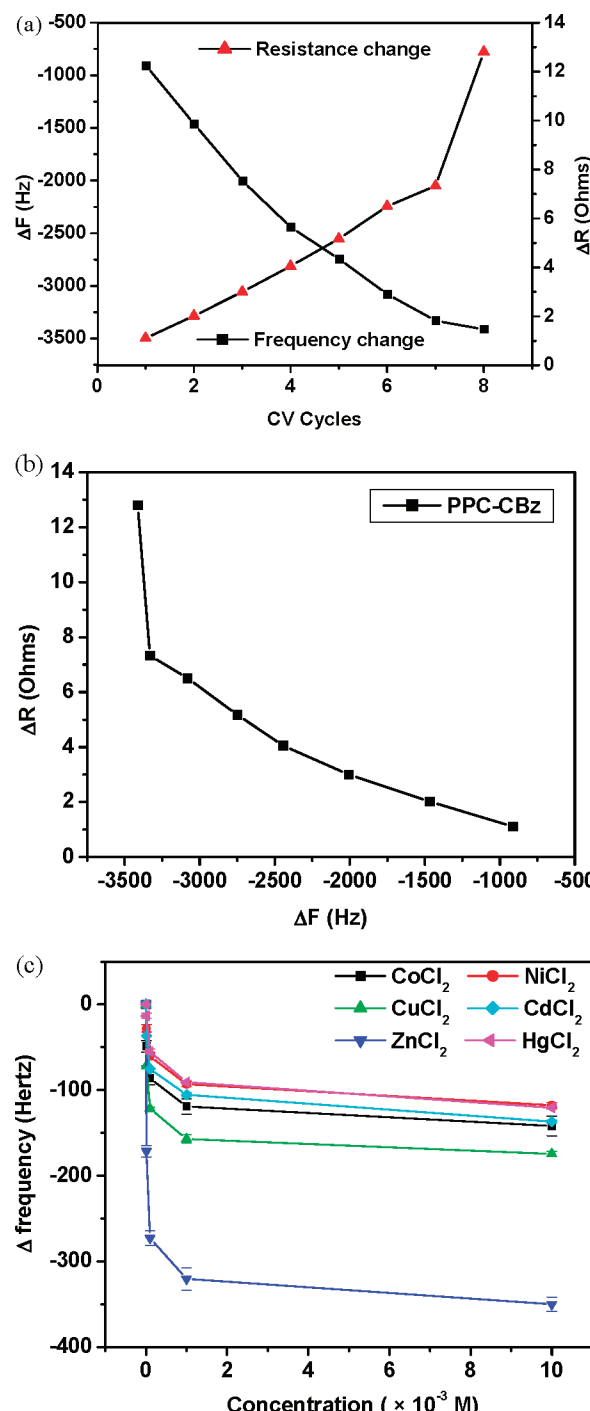


Figure 6. Electrochemical quartz crystal microbalance studies the following: (a) ΔF , frequency change, and ΔR , resistance change during the CV cycling. (b) Changes in the viscoelastic behavior in the polymers. (c) ΔF , frequency change as a function of different cations concentration.

as follows: Zn^{2+} ($K = 1.1 \times 10^6 \text{ M}^{-1}$) $>$ $\text{Cu}^{2+} \approx \text{Co}^{2+}$ ($K = 9.0 \times 10^5 \text{ M}^{-1}$) $>$ $\text{Ni}^{2+} \approx \text{Hg}^{2+}$ ($K = 3.3 \times 10^5 \text{ M}^{-1}$) $>$ Cd^{2+} ($K = 2.5 \times 10^5 \text{ M}^{-1}$).

Finally, SPR spectroscopy was combined with an electrochemistry setup to study the efficiency of transport and sensitivity of Zn^{2+} ions with PPC-CBz films. As shown in the EC-SPR measurements (Figure 7), the reflectivity increases with increasing CV cycles, indicating the continuous deposition of the film onto the 4 SAM coated gold substrates. Again, the subsequent doping and dedoping of the films with oxidation and reduction cycles are shown in

(17) Buttry, D. A.; Ward, M. D. *Chem. Rev.* **1992**, *92*, 1355.
 (18) Muramatsu, H.; Tamaya, E.; Karube, I. *Anal. Chem.* **1988**, *60*, 2142.
 (19) Sannicolo, F.; Brenna, E.; Benincori, T.; Zotti, G.; Zecchin, S.; Schiavon, G.; Pilati, T. *Chem. Mater.* **1998**, *10*, 2167.

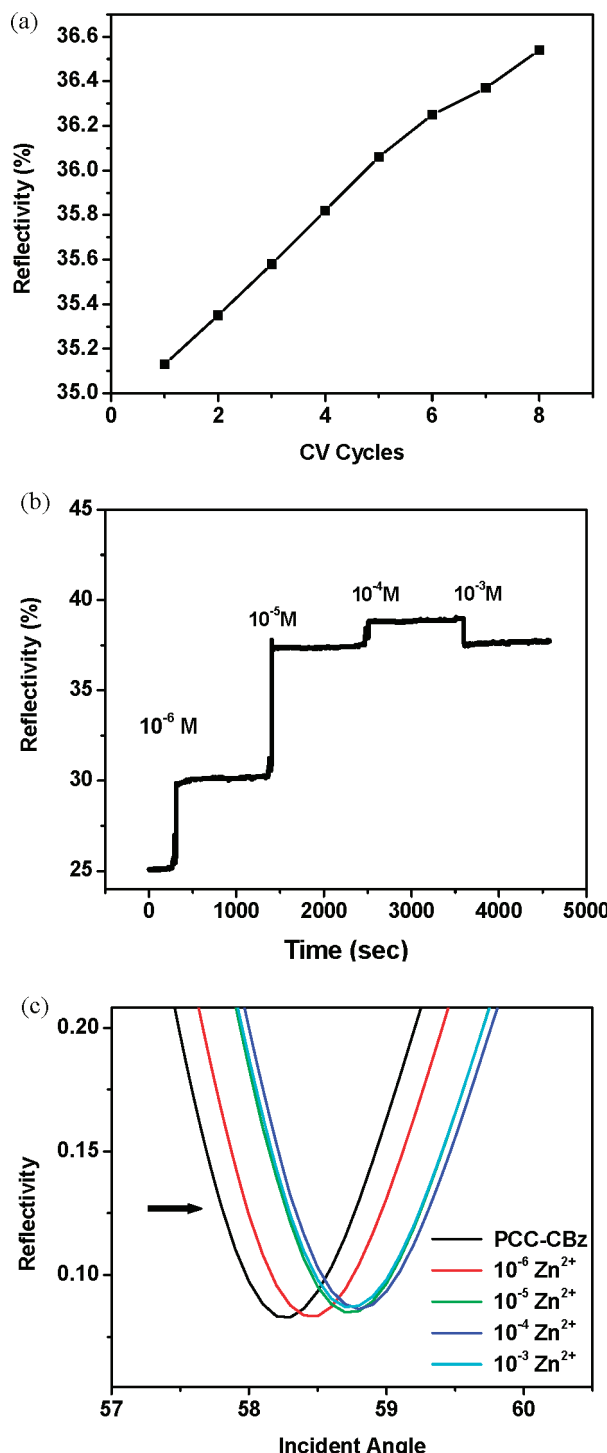


Figure 7. EC-SPR and SPR studies of PPC-CBz on **4** coated gold substrates: (a) kinetic measurement during deposited film, (b) kinetic sensorgram at different concentrations of Zn^{2+} , and (c) angular sensorgram at different concentrations of Zn^{2+} .

the reversible reflectivity change which consists of either a change in dielectric constant or thickness.²⁰

The sensing experiment was conducted by injecting different concentrations of Zn^{2+} into the SPR cell embedded with the as-deposited polymer film on a Au working electrode. From

(20) (a) Taraneckar, P.; Baba, A.; Park, J. Y.; Fulghum, T. M.; Advincula, R. *Adv. Funct. Mater.* **2006**, *16*, 2000. (b) Kang, X.; Jin, Y.; Cheng, G.; Dong, S. *Langmuir* **2002**, *18*, 10305. (c) Georgiadis, R.; Peterlinz, K. A.; Rahn, J. R.; Peterson, A. W.; Grassi, J. H. *Langmuir* **2000**, *16*, 6759. (d) Bund, A.; Baba, A.; Berg, S.; Johannsmann, D.; Lubben, J.; Wang, Z.; Knoll, W. *J. Phys. Chem. B* **2003**, *107*, 6743.

the SPR sensorgram (Figure 7b), a sudden change was observed on the reflectivity upon injection of 10^{-6} and 10^{-5} M Zn^{2+} and a peak saturation was observed upon injection of 10^{-4} M and higher concentrations. The concentrations at this level are not expected to give a measurable change in reflectivity.²¹ This indicated that the association of Zn^{2+} with the film induced primarily the dielectric constant change assuming the thickness was constant. It is also interesting to note that the highest change was observed with 10^{-6} and 10^{-5} M Zn^{2+} concentrations, indicating that at these concentrations the azacalix[3]arene units are fully bounded and that excess ions do not participate in a significant dielectric constant change to the film, similar to the results with open-circuit potentiometry. This confirms that the allosteric effect is mostly observed only at lower concentrations of the Zn^{2+} cation and that, at higher concentrations, the excess ion does not participate in binding to the azacalix[3]arenes.

Conclusion

In summary, we have successfully developed a new class of chemosensor recognition elements based on conjugated polymer network ultrathin films by electrochemical cross-linking of hexahomotriazacalix[3]arene–carbazole and demonstrated its selectivity and sensitivity toward Zn^{2+} by various techniques: potentiometry, QCM, and SPR combined with electrochemistry. The results of this investigation have shown that cation interaction with the film might increase charge carrier transport properties on a conjugated polymer through azacalix[3]arene-bound cations, reduce the doping states by interfering ions through ion–ion interaction, and perturbing the π -extended conjugated polymer through π – π interaction. Specifically, these observed changes in the electrical and spectroelectrochemical properties of the films are related to the cation–dipole interaction between Zn^{2+} and azacalix[3]arene, resulting in a higher binding constant and its subsequent specificity for chemical sensing.

Experimental Section

Chemicals and Methods. All chemical reagents were purchased from Aldrich Chemical Co. unless otherwise stated. Solvents were purchased from Fisher. Tetrahydrofuran (THF) was distilled over sodium/benzophenone ketyl, and *N,N*-dimethylformamide (DMF) was purchased in anhydrous form or was otherwise dried over Linde type 4 Å molecular sieves.

Instrumentation. Nuclear magnetic resonance (NMR) spectra were recorded on a Varian 400 MHz spectrometer in deuterated chloroform or a General Electric QE-300 spectrometer at 300 MHz. Chemical shifts (δ) are reported in parts per million and the residual solvent peak was used as an internal standard.

UV-vis spectra were recorded using an HP-8453 spectrometer. Spectroelectrochemical UV-vis measurements of the films were carried out *in situ* on ITO substrates. This was done using a Teflon flow cell fabricated with a modified ITO window and microscope slide window that was placed in the path of an HP-8453 diode array spectrometer.

MALDI-TOF mass spectra were recorded on a Biflex Bruker Mass spectrometer with 2-cyano-4-hydroxycinnamic acid (CCA) or 2,5-dihydroxybenzoic acid (DHB) as matrix.

(21) Neumann, T.; Johansson, M.-L.; Kambhampati, D.; Knoll, W. *Adv. Funct. Mater.* **2002**, *12*, 575.

All FTIR measurements were performed using a Digilab FTS 7000 step scan spectrometer.

The cyclic voltammetry (CV) experiments were carried out on a Princeton Applied Research Parstat 2263 with a modified ITO substrate as the working electrode coupled with a Pt plate counter and Ag/AgCl reference electrode. Cyclic voltammetry was utilized to prepare the cross-linked films from a 0.1 wt % of the precursor polymer solution of 0.1 M TBAPF₆/CH₂Cl₂.

The QCM apparatus, probe, and crystals are available from Maxtek Inc. The data acquisition was done using a RQCM (Research Quartz Crystal Microbalance, Maxtek, Inc.) system equipped with a built-in phase lock oscillator and the RQCM Data-Log Software. This was coupled with the Amel potentiostat to generate EC-QCM results. A 5 MHz AT-cut CBzC11SH modified on Au-coated quartz crystal with an effective area of 1.327 cm² was used as a working electrode. Platinum as a counter electrode and Ag/AgCl as a reference were used to measure *in situ* polymerization during cyclic voltammetry. To initiate the experiment, an inert probe was first immersed in methylene chloride until a stable frequency was obtained.

Surface plasmon resonance spectroscopy (SPR) on Au-coated glass (~45 nm) was performed using a commercially available instrument (Multiskop) with a Kretschmann configuration and attenuated total reflection (ATR) conditions.¹⁴ The reflectance was monitored with a p-polarized He–Ne laser (632.8 nm) as a function of angle of incidence.

Electrochemical surface plasmon resonance spectroscopy (EC-SPR) measurements were performed using a SPR setup combined with a three-electrode electrochemical cell in a Kretschmann configuration for the excitation of surface plasmons. The details of this setup are described in the Supporting Information. Surface plasmons were excited by reflecting p-polarized laser light off the Au-coated base of the prism. The excitation source employed was a He–Ne laser: $\lambda = 632.8$ nm. Kinetic measurements were performed to monitor the formation of the film. Reflectivity-angular measurements were also performed by scanning an incident angle range before and after *in situ* polymerization. For these experiments, the gold film thickness (~45 nm) was chosen for optimum excitation of the surface plasmons. The electrode surface area was 0.785 cm².

Atomic force microscopy (AFM) imaging was examined in ambient conditions with a PicoSPM II (PicoPlus System, Molecular Imaging (now Agilent Technologies) Tempe, AZ) in tapping mode (AAC mode).

Synthesis. *Synthesis of 9-(Undec-10-enyl)-9H-carbazole (2).* To a stirred solution of 6.00 g (36.00 mmol) of carbazole in 15 mL of dimethylformamide (DMF), NaH 1.83 g (39.6 mmol) was added in portions, and after complete addition the mixture was heated to 60 °C for 2 h. After the mixture was cooled, a solution of 11-bromoundec-1-ene (9.40 g, 40.00 mmol) in 5 mL of DMF was added dropwise to the reaction mixture and was allowed to stir for 48 h at room temperature. The reaction mixture was then poured into water, extracted using methylene chloride, and dried over anhydrous Na₂SO₄. After the solvent was evaporated, the crude product was purified by column chromatography; using hexane as an eluent gave 9.50 g (3%) of the product. ¹H NMR (300 MHz, CDCl₃): δ 8.14 (d, $J = 7.8$ Hz, 2H, ArH), 7.53–7.42 (m, 4H, ArH), 7.27 (t, $J = 7.4$ Hz, 2H, ArH), 5.84–5.63 (m, 1H, CH₂CH=CH₂), 4.99–4.82 (m, 2H, CH₂CH=CH₂), 4.29 (t, $J = 6.6$ Hz, 2H, NCH₂CH₂), 2.17–1.93 (m, 2H, CH₂CH₂CH), 1.96–1.67 (m, 2H, CH₂CH₂CH₂), 1.35–1.22 (m, 12H, CH₂CH₂CH₂). ¹³C NMR (75 MHz, CDCl₃): 140.6, 139.3, 125.7, 123.1, 120.3, 118.9, 114.3, 109.9, 43.4, 34.2, 29.8, 29.7, 29.4, 29.3, 29.2, 27.7.

Synthesis of 11-(9H-Carbazol-9-yl)undecyl Ethanethioate (3). A solution of **2** (1.91 g, 6.00 mmol) in dry tetrahydrofuran (THF, 20 mL) containing thioacetic acid (0.63 g, 8.32 mmol) and 2,2'-azobis(2-methylpropionitrile) (AIBN) (56 mg, 0.172 mmol) was refluxed at 60 °C for 12 h under nitrogen. After cooling of the reaction flask, 20 mg of AIBN and 0.30 g of thioacetic acid were added and the mixture was refluxed for another 4 h. Concentration of the reaction mixture followed by flash column chromatography (4:1 hexane/CH₂Cl₂) gave 2.10 g (89%) of the product. ¹H NMR (300 MHz, CDCl₃): δ 8.14 (d, $J = 7.8$ Hz, 2H, ArH), 7.53–7.42 (m, 4H, ArH), 7.27 (t, $J = 7.8$ Hz, 2H, ArH), 4.29 (t, $J = 6.8$ Hz, 2H, NCH₂CH₂), 2.70 (t, $J = 6.8$ Hz, 2H, CH₂CH₂CO), 2.35 (s, 3H, COCH₃), 1.92–1.88 (m, 2H, CH₂CH₂CH₂), 1.74–1.69 (m, 2H, CH₂CH₂CH₂), 1.38–1.26 (m, 14H, CH₂CH₂CH₂). ¹³C NMR (75 MHz, CDCl₃): 196.0, 140.6, 125.7, 123.1, 120.3, 118.6, 108.9, 43.0, 39.1, 35.1, 32.1, 30.5, 29.4, 29.3, 29.1, 28.9, 27.3.

Synthesis of 11-(9H-Carbazol-9-yl)-undecane-1-thiol (4). In a 100 mL round-bottomed flask, **3** (1.00 g, 2.52 mmol) was dissolved in 10 mL of methanol, and CH₂Cl₂ was added dropwise to make the suspension clear. To this solution was added 1 mL of 50 wt % NaOH under nitrogen and the resulting mixture was allowed to stir overnight. The reaction mixture was neutralized by the addition of acetic acid. The neutralized solution was then poured into 25 mL of water and the organic phase was extracted using methylene chloride. The organic phase was then washed with brine and dried over Na₂SO₄. After filtration and concentration under vacuum, the crude product was further washed with hexane to give the pure product as 0.78 g (87%) of slightly yellowish oil. ¹H NMR (300 MHz, CDCl₃): δ 8.14 (d, $J = 7.8$ Hz, 2H, ArH), 7.53–7.42 (m, 4H, ArH), 7.27 (t, 2H, ArH), 4.29 (t, 2H, NCH₂CH₂), 2.68 (t, 2H, CH₂CH₂SH), 1.92–1.88 (m, 2H, CH₂CH₂CH₂), 1.74–1.69 (m, 2H, CH₂CH₂CH₂), 1.38–1.26 (m, 15H, CH₂CH₂CH₂ and SH). ¹³C NMR (75 MHz, CDCl₃): 140.6, 125.7, 123.1, 120.3, 118.6, 108.9, 43.0, 39.1, 35.1, 32.1, 29.3, 29.1, 29.0, 28.9, 28.4, 27.3.

Synthesis of 4-Chloro-2,6-bis(hydroxymethyl)phenol (5).^{6e} To a solution of *p*-chlorophenol were added formaldehyde and sodium hydroxide and the resulting mixture was stirred for 7–10 days. The sodium salts of **5** were isolated by removal of the solvent under reduced pressure. Acidification of the sodium salts with acetic acid in acetone, removal of sodium acetate by filtration, and recrystallization from ethyl acetate resulted in 72% yield. ¹H NMR (400 MHz, CD₃OD): 7.178 (s, 2H, ArH), 7.3 (m, 6H, ArH). IR (KBr): ν 3412, 3300, 2967, 2914, 2888, 1478, 1456, 1211, 1068, 1010 cm⁻¹. MS (MALDI-TOF) Calcd for [C₈H₉ClO₃]⁺: *m/z* 188.02. Found: *m/z* 189 [M + H]⁺.

Synthesis of p-Chloro-N-benzylhexahomotriazacalix[3]arene (6).^{6e} To a solution of **5** (6.00 g, 32.52 mmol) was added benzylamine (3.39 g, 31.67 mmol) in 150 mL of xylene; the resulting mixture was refluxed for 72 h, and the water generated was removed during the course of the reaction with a Dean-Stark condenser. The mixture was evaporated to dryness as deep yellow oil. Chromatography on silica gel (hexane:EtOAc = 9:1, v/v) gives **6** (2.73 g, 33% yield). ¹H NMR (400 MHz, CD₂Cl₂): δ 7.29 (br s, 15H, ArH), 7.01 (s, 6H, ArH), 3.69 (s, 6H, NCH₂Ar), 3.64 (s, 12H, NCH₂Ar). ¹³C NMR (100 MHz, CDCl₃): δ 155.5, 136.4, 129.6, 129.4, 128.1, 127.3, 125.0, 122.7, 58.0, 56.7. IR (KBr): ν 3054, 3023, 2832, 2805, 1738, 1602, 1470, 1372, 1240, 1116, 863, 738, 699, 485 cm⁻¹. MS (MALDI-TOF) Calcd for [C₄₅H₄₂C₁₃N₃O₃]⁺: *m/z* 777.23. Found: *m/z* 778.69 [M + H]⁺. Anal. Calcd for C₄₅H₄₂C₁₃N₃O₃: C, 69.36; H, 5.43; N, 5.39. Found: C, 65.48; H, 5.78; N, 9.38.

Synthesis of 9-(4-Bromobutyl)-9H-carbazole (7). A solution of 59.1 g (237.7 mmol) of 1,4-dibromobutane, 1.00 g of tetrabutylammonium bromide, 5.16 g (30.86 mmol) of carbazole, 50 mL of

aqueous 50% sodium hydroxide, and 50 mL of benzene was stirred at 40 °C for 6 h. The organic layer was separated, and the aqueous layer was extracted three times with chloroform (3 × 30 mL). The combined organic layer was washed three times with water (3 × 40 mL) and dried over Na₂SO₄. The organic solvent was distilled over a water bath, the unreacted 1,4-dibromobutane was removed by vacuum distillation, and the residue was recrystallized from ethanol to give a white needle-like solid. Yield: 5.8 g (62%). ¹H NMR (300 MHz, CDCl₃): δ 8.06 (d, 2H, ArH), 7.11–7.47 (m, 6H, ArH), 4.29 (t, *J* = 5.4 Hz, 2H, NCH₂), 3.32 (t, *J* = 5.8 Hz, 2H, CH₂CH₂Br), 1.98 (m, 4H, ArCH₂CH₂). IR (KBr): ν 3045, 2939, 2925, 2855, 1620, 1593 cm⁻¹.

Synthesis of p-Chloro-N-benzylhexahomotriazacalix[3]-tri(butyl-carbazole) (1). To a solution of **6** (0.50 g, 0.64 mmol), NaH (0.11 g, 4.42 mmol) in THF (20 mL), and DMF (5 mL) was added a solution of **7** (0.68 g, 2.25 mmol) in THF (10 mL). After being stirred for 2 days at 80 °C, the reaction mixture was evaporated, extracted with CH₂Cl₂, and washed with saturated NaHCO₃. The organic layer was dried over anhydrous Na₂SO₄, filtered, and evaporated under vacuum. Column chromatography on silica gel (hexane/EtOAc = 9:1, v/v) afforded **1** (0.09 g, 0.06 mmol) in 10% yield as deep white oil. ¹H NMR (300 MHz, CDCl₃): δ 8.13–8.11 (m, 6H, ArH_{cbz}), 7.52–7.48 (m, 12H, ArH_{cbz}), 7.31 (m, 15H, ArH_{calix}), 7.04 (s, 4H, ArH_{calix}), 7.01 (s, 2H, ArH_{calix}), 4.13 (t, *J* = 7.2 Hz, 2H, OCH₂CH₂), 3.74 (t, *J* = 7.2 Hz, 4H, OCH₂CH₂), 3.78–3.00 (m, 24H, NCH₂Ar and CH₂CH₂N_{cbz}), 1.76–1.18 (m, 12H, CH₂CH₂CH₂). ¹³C NMR (75 MHz, CDCl₃): δ 157.5, 155.5, 141.0, 140.9, 139.8, 139.7, 135.0, 134.0, 133.6, 131.4, 129.9, 129.5, 129.4, 129.1, 128.9, 127.9, 127.7, 126.2, 123.4, 121.0, 120.9, 119.5, 119.4, 119.3, 109.3, 109.2, 75.0, 74.7, 63.4, 62.8, 60.4, 53.2, 52.2, 51.4, 43.50, 43.3, 30.2, 28.2, 28.1, 26.3, 26.2. IR (KBr): ν 2977, 2937, 2880, 1470, 1386, 1320, 1243, 1168, 1107, 1059, 1035, 929, 879, 817, 738 cm⁻¹. MS (MALDI-TOF) Calcd for [C₉₃H₈₇Cl₃N₆O₃]⁺: *m/z* 1443.08. Found: *m/z* 1443.70 [M + H]⁺.

Synthesis of 9-(4-(9H-carbazol-9-yl)butyl)-9H-carbazole (8). A solution of carbazole (5.00 g, 30.00 mmol) and KOH (1.68 g, 30.00 mmol) in acetone (20 mL) was added dropwise into a solution of dibromobutane (2.60 g, 12.00 mmol) in acetone (5 mL). After being stirred for 24 h at RT, the reaction mixture was evaporated, then extracted with CH₂Cl₂, and finally washed with EtOH and THF. The filter was dried in vacuum to afford **3** (3.26 g, 8.39 mmol) in 70% yield as a white solid. ¹H NMR (300 MHz, CDCl₃): δ 8.10 (d, *J* = 7.7 Hz, 4H, ArH), 7.45–7.43 (m, 4H, ArH), 7.23 (m, 4H, ArH), 4.24 (t, *J* = 7.2 Hz, 4H, NCH₂CH₂), 2.13–1.88 (m, 4H, CH₂CH₂CH₂).

Electrochemical Synthesis of Cross-linked Polymers (PPC-CBZ). The precursor polymers were synthesized using the cyclic voltammetry (CV) technique. In a three-electrode cell, 0.1 M tetrabutylammonium hexafluorophosphate (TBAPF₆) was used as a supporting electrolyte along with 0.1 wt % precursor **1** dissolved in anhydrous methylene chloride in separate cells. The electropo-

lymerization of each precursor **1** was performed by sweeping the voltage at a scan rate of 50 mV/s from 0 to 1.0, 1.3, 1.5 V against Ag/AgCl as a reference electrode and platinum as a counter electrode. The ITO, gold-coated slides, and **4** coated gold substrates were used both as a working electrode and as a substrate.

Sensitivity and Selectivity Studies of PPC-CBz by Using Potentiometry. Polymerized on ITO substrates by sweeping the voltage at a scan rate of 50 mV/s from 0 to 1.3 V, **1** was studied as a sensor using 0.01 M TBACl as electrolyte. With use of a Teflon cell, 0.01 M TBACl was injected, until the potential signal was kept constant. To study sensitivity and selectivity of the polymer, different concentrations of cations were held constant for 1000 s. The change in potential (ΔE), [ΔE] = observed potential (E_0) – initial potential (E_i) was recorded simultaneously as a function of time.

Sensitivity and Selectivity Studies of PPC-CBz by Using EC-QCM and QCM. EC-QCM was used to polymerize PC-CBz on **4** coated gold substrates. The electropolymerization was performed by sweeping the voltage at the scan rate of 50 mV/s from 0 to 1.0 V. The sensitivity and selectivity were monitored in aqueous solution. From Figure S1, we injected water into the sample cell and kept this cell constant at room temperature for 1000 s. After that, such cell was dried in a vacuum oven for 10 min, and each delta frequency shown in Figure S1 was measured in air by QCM each time for 20 min as a function of cations' concentration: 10⁻⁶, 10⁻⁵, 10⁻⁴, and 10⁻³ M.

Sensitivity and Selectivity Studies of PPC-CBz by Using EC-SPR and SPR. The details of this setup are described in Figure S2. Electropolymerization was done by EC-SPR (WE, **4** coated gold substrates; CE, Pt wire; RE, Ag/AgCl) at a scan rate of 20 mV/s (0 to 1.0 V). The sensing experiment was performed by injecting different concentrations of cations and each concentration stood for 1000 s at room temperature. Kinetic and angular measurements were observed as a function of time.

Acknowledgment. The authors gratefully acknowledge financial support from NSF-DMR (05-04435), NSF-DMR-(06-02896), NSF-CTS (0330127), and the Robert A. Welch Foundation. C.K. and B.P. acknowledge support from the Thailand Research Fund (TRF) (RMU4880041) and the Royal Golden Jubilee Ph.D Program of TRF (PHD/0137/2546). We also acknowledge Prof. Akira Baba for his assistance in setting up the surface plasmon resonance spectrometer. Technical support from Maxtek Inc. and Optrel GmbH is also acknowledged.

Supporting Information Available: Experimental details and results for electrochemistry and AFM analysis on other substrates and control experiments for sensing (PDF). This material is available free of charge via the Internet at <http://pubs.acs.org>.

CM800284H